Grafted versus Non-Grafted Polymer Adsorption

Monika Möddel[1]**, Michael Bachmann**[2,3]**, and Wolfhard Janke**[1]

[1] Institut für Theoretische Physik and Centre for Theoretical Sciences (NTZ), Universität Leipzig
Postfach 100 920, D-04009 Leipzig, Germany
E-mail: {Monika.Moeddel, Wolfhard.Janke}@itp.uni-leipzig.de

[2] Center for Simulational Physics, The University of Georgia, Athens, GA 30602, U.S.A.
E-mail: bachmann@smsyslab.org

[3] Institute for Complex Systems (ICS-2) and Institute for Advanced Simulation (IAS-2)
Forschungszentrum Jülich, D-52425 Jülich, Germany

The conformational behaviour of a semi-flexible self-interacting finite polymer near an attractive substrate was investigated with the parallel tempering Monte Carlo method. This method allows for a precise estimate of canonical equilibrium data over a wide range of surface attraction strengths and temperatures, which enables us to identify the different phases of the finite system via thermal fluctuations of canonical expectation values of energetic and structural quantities. Complementary microcanonical information is extracted from the density of states. The resulting phase diagrams for grafted and non-grafted polymers are discussed and compared.

1   Introduction

In a diluted polymer solution extended polymer conformations are favoured at high temperatures due to their higher conformational entropy compared to globular conformations. Reducing the temperature, globular conformations gain thermodynamic weight, and the polymer collapses in a cooperative rearrangement of the monomers. Those globular conformations are relatively compact but have only little internal structure. Hence, they are still entropy-dominated, and a further transition towards low-degenerate crystalline energetic states is expected and indeed observed: the freezing transition[1,2]. Although it has been shown that these two transitions fall together for sufficiently short-range interactions[3], they are clearly distinct in general.

The presence of an attractive substrate modifies this behaviour of the polymer and gives rise to theoretical and computational challenges. It not only adds the adsorption transition, but also induces several phases by the competition between monomer-monomer and monomer-surface attraction. Although the properties of some phases and subphases depend on the exact number of monomers, they are not less interesting, because with the advent of new sophisticated experimental techniques such small scales become accessible. Among such techniques at the nanometer scale is, e.g., atomic force microscopy (AFM), where it is possible to measure the contour length and the end-to-end distance of individual polymers[4] or to quantitatively investigate the peptide adhesion on semiconductor surfaces[5]. Another experimental tool with an extraordinary resolution in positioning and accuracy in force measurements are optical tweezers[6,7].

Numerous detailed numerical studies have been performed to elucidate the conformational behaviour of homopolymers and heteropolymers near substrates. Compared to experiments, computer simulations have the advantage that a wide range of control parameters can be scanned at will. Theoretical studies have, e.g., been performed analytically

using scaling theory[8,9], mean-field density functional theory[10], and series expansions[11] and numerically by employing off-lattice models such as a bead-spring model of a single polymer chain grafted to a weakly attractive surface[12,13], Monte Carlo studies of lattice homopolymers[8,12,14–17], or exact enumeration[18] to name only a few.

Our focus here is on the classification of thermodynamic phases and phase transitions for a range of surface attraction strengths and temperatures and we compare the results for end-grafted polymers with those of non-grafted polymers that can move freely within a simulation box. After we recently constructed such a phase diagram for the non-grafted case[19], and also analyzed the influence of the simulation box size[20], the question arises whether there is a qualitative difference between grafted and non-grafted adsorption. This gap of a systematic comparison of both cases using an otherwise identical coarse-grained model shall be filled here[21]. The reduction of degrees of freedom speeds up the simulation considerably, but still the problem is computationally very demanding, such that the well established parallel tempering Monte Carlo (MC) method with MPI is applied. This allows for an easy and efficient parallelization on the Jülich supercomputer JUROPA.

2 Model

The model used here is a simple bead-stick model of a linear polymer with three terms that contribute to the energy[19,20],

$$E = 4 \sum_{i=1}^{N-2} \sum_{j=i+2}^{N} \left(r_{ij}^{-12} - r_{ij}^{-6} \right) + \frac{1}{4} \sum_{i=1}^{N-2} \left(1 - \cos \vartheta_i \right) + \epsilon_s \sum_{i=1}^{N} \left(\frac{2}{15} z_i^{-9} - z_i^{-3} \right), \quad (1)$$

where the first two terms are the energy in bulk that consists of the standard 12-6 Lennard-Jones (LJ) potential and a weak bending energy. The distance between the monomers i and j is r_{ij} and $0 \leq \vartheta_i \leq \pi$ denotes the bending angle between the ith, $(i+1)$th, and $(i+2)$th monomer. The third term is the attractive surface potential, obtained by integration over the continuous half-space $z < 0$ (cf. Fig. 1), where every space element interacts with a single monomer by the 12-6 LJ expression[22]. Hence, the parameter ϵ_s weighs the monomer-surface and monomer-monomer interaction. We use generic units, in which $k_B = 1$.

The relative strength of the two interactions is continuously varied by considering ϵ_s as a control parameter. We simulate the polymer once grafted with one end to the substrate in the potential minimum and once freely moving in the space between the substrate and a hard wall a distance $L_z = 60$ away. To describe the system, we measure several canonical expectation values $\langle O \rangle$,
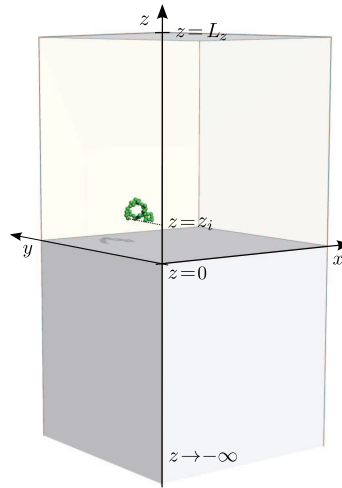

Figure 1. Graphical representation of the system of a single polymer close to an attractive substrate at $z = 0$. The hard wall at $z = L_z$ prevents a non-grafted polymer from escaping.

determine their temperature derivative and also keep a look at their microcanonical behaviour with energy $O(E)$ and the density of states $g(E)$. The most basic observable O is the energy E itself, whose temperature derivative is the specific heat $c_V(T)$. The squared radius of gyration $R_{\mathrm{gyr}}^2 \equiv \sum_{i=1}^{N}(\vec{r}_i - \vec{r}_{\mathrm{cm}})^2$, with $\vec{r}_{\mathrm{cm}} = (x_{\mathrm{cm}}, y_{\mathrm{cm}}, z_{\mathrm{cm}}) = \sum_{i=1}^{N}\vec{r}_i/N$ being the centre-of-mass of the polymer, as a measure for the extension of the polymer as well as its tensor components parallel and perpendicular to the substrate, $R_{\parallel}^2 = \sum_{i=1}^{N}[(x_i - x_{\mathrm{cm}})^2 + (y_i - y_{\mathrm{cm}})^2]$ and $R_{\perp}^2 = \sum_{i=1}^{N}(z_i - z_{\mathrm{cm}})^2$, offer rich information since the substrate introduces a structural anisotropy into the system. One indicator for adsorption is the distance of the centre-of-mass of the polymer to the surface. Additionally, we analyze the mean number of monomers docked to the surface n_s. For the continuous substrate potential we define a monomer i to be docked if $z_i < z_c \equiv 1.5$.

3 Methods

To simulate this model system, the parallel tempering or replica exchange MC method[23, 24] is applied. The basic idea is to run several Metropolis simulations in parallel at different inverse temperatures $\beta_1 < \ldots < \beta_n = 1/T_n$. Every once in a while two copies of the system exchange their current conformations with the Metropolis acceptance probability

$$A(\mu\nu \to \nu\mu) = \min\left(1, \frac{p_{\nu\mu}}{p_{\mu\nu}}\right) = \min\left(1, e^{\Delta\beta\Delta E}\right), \tag{2}$$

where $p_{\mu\nu} = e^{-\beta E_\mu}Z_\beta^{-1}e^{-\beta' E_\nu}Z_{\beta'}^{-1}$ is the joint probability of the systems at β and β' to be in state μ and ν, respectively. Z_β and $Z_{\beta'}$ are the associated canonical partition functions. This way conformations that were stuck in a valley of the energy landscape at low temperatures can escape at higher temperatures and eventually explore other regions of phase space. Such an approach combines two important advantages. It strongly decreases the autocorrelation time at low temperatures and is highly parallelizable.

In the case of a large temperature separation of the two replicas that attempt an exchange of their conformations, the acceptance probability gets small. Hence, for the performance of this method both, the number and the temperatures of the replicas are essential. In order that two replicas exchange their conformations, their energy histograms have to have a sufficient overlap as can be seen from Eq. 2. If one is interested in low-temperature properties, the range from those low temperatures to high enough temperatures to cross free energy barriers has to be covered. This sets a minimum of necessary replicas. Choosing too many, on the other hand, slows down the simulation effectively, since it takes longer on average for a replica to go from low to high temperatures and back again. There exist several attempts to optimize the choice of the β_i,[25] but usually one can get a reasonable performance when observing the histograms and ensuring the acceptance probability to be around 50%, which approximately requires an equidistribution in β. Here, 64-72 different replicas are used with 50 000 000 sweeps each, from which every 10th value was stored in a time series – the autocorrelation time in units of sweeps is of the order of thousands. For the canonical analysis, this statistics is very generous, but to obtain data with low statistical errors for the microcanonical entropy $S(E) = \ln g(E)$ and its derivatives, higher precision data are necessary. This was done for $\epsilon_s = 0, 0.1, \ldots, 5$.
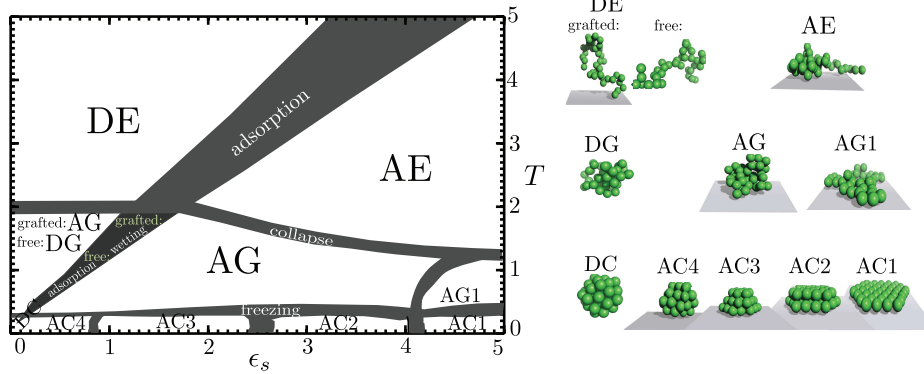
Figure 2. The pseudo-phase diagram parametrized by adsorption strength ϵ_s and temperature T for a 40mer. The purple transition regions have a broadness that reflects the variation of the corresponding peaks of the fluctuations of canonical expectation values we investigated. Phases with an "A/D" are adsorbed/desorbed. "E", "G" and "C" denote phases with increasing order: expanded, globular and compact/crystalline. The right panel shows representative conformations of the individual phases.

After having performed this simulation, one is confronted with the problem of how to combine all those canonical histograms $H_i(E)$, $i = 1, \ldots, n$, to get an optimal combination of the data available[26]. We use an error-weighted histogram reweighting method similar to the one in Ref. 27. All histograms $H_i(E)$ can be reweighted to yield an estimate of the density of states at inverse temperatures β_i, $g_i(E) \propto H_i(E)e^{\beta_i E}$, that is only of reasonable quality in an energy regime with sufficient statistics. Since absolute estimates of the partition function cannot be obtained in MC simulations, there is an unknown prefactor that is different for every β_i. To get rid of it, we work with the ratio $g_i(E + \Delta E)/g_i(E)$ and since $g(E)$ spans many orders of magnitude, it is advantageous to use the logarithm:

$$\Delta S_i(E) = S_i(E + \Delta E) - S_i(E) = \ln\left[g_i(E + \Delta E)/g_i(E)\right]$$
$$= \ln\left[H_i(E + \Delta E)\right] - \ln\left[H_i(E)\right] + \beta_i \Delta E. \tag{3}$$

Now, an error-weighted average over all histograms,

$$\overline{\Delta S}(E) = \frac{\sum_i \Delta S_i(E) w_i(E)}{\sum_i w_i(E)}, \tag{4}$$

can be taken with $w_i(E) = 1/\sigma^2(\Delta S_i(E)) \simeq [H_i(E + \Delta E)H_i(E)]/[H_i(E + \Delta E) + H_i(E)]$. This gives an excellent estimate of $\beta(E) \approx \overline{\Delta S}(E)/\Delta E$ as long as all histograms overlap – which parallel tempering requires anyway. Up to a constant, the microcanonical entropy $S(E)$ is obtained by integration.

4   Results

All transitions are contained in the phase diagram for a 40mer in Fig. 2. It is constructed using the profile of several canonical fluctuations as shown for the specific heat in Fig. 3. A strong difference between the grafted and non-grafted case is observed at the adsorption transition, while the other transitions remain more or less unaffected.
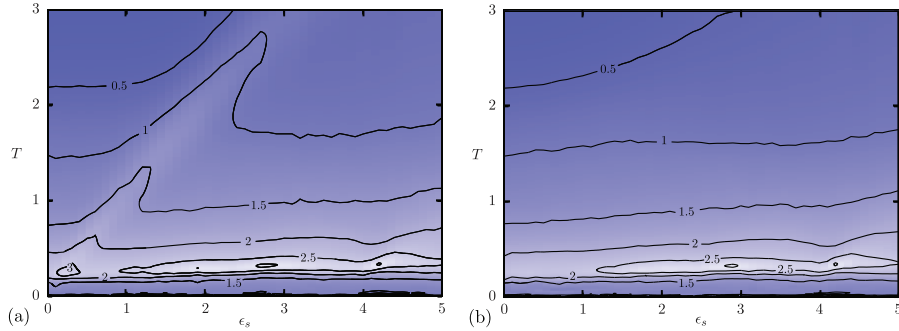
Figure 3. Specific-heat profile, $c_V(\epsilon_s, T)$, for (a) the non-grafted and (b) the grafted polymer.

Non-Grafted Polymer. The specific heat for the non-grafted polymer in Fig. 3(a) clearly reveals the freezing and adsorption transitions. The freezing leads to a pronounced peak near $T = 0.25$ almost independently of the surface attraction strengths. That this is indeed the freezing transition is confirmed by the very rigid crystalline structures found below this temperature and the rapidly decreasing density of states in the corresponding energy regime [cf. Fig. 4(a)].

To differentiate between the different crystalline structures, the radius of gyration, its tensor components parallel and perpendicular to the substrate, and the number of surface contacts were analyzed. This revealed that the crystalline phases arrange in a different number of layers to minimize the energy. For high surface attraction strengths, a single layer is favoured (AC1), and for decreasing ϵ_s the number of layers increases until for the 40mer a maximal number of 4 layers is reached (AC4), cf. Fig. 2. The fewer layers are involved in any layering transition, the more pronounced is that transition.

Raising the temperature above the freezing temperature, polymers form adsorbed and still rather compact conformations. This is the phase of adsorbed globular (AG) conformations that can be subdivided into drop-like globules for ϵ_s that are not strong enough to induce a single layer below the freezing transition and more pancake-like flat conformations (AG1) at temperatures above the AC1 phase. At even higher temperatures, two scenarios can be distinguished. In the first case, the polymer first desorbs from the sur-
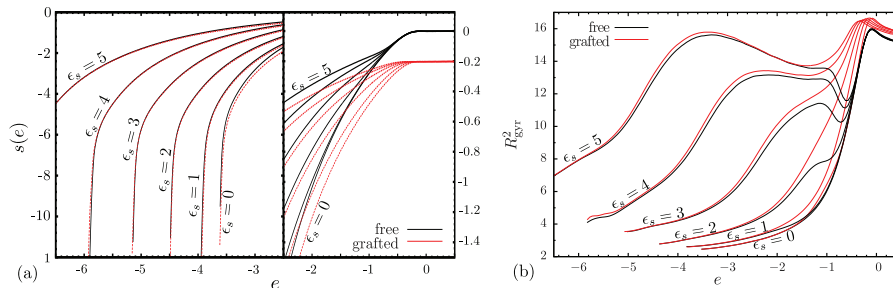

Figure 4. (a) Microcanonical entropy $s(e) = \ln g(e)/N$. Since $g(e)$ spans many orders of magnitude at low energies, the ordinate is divided into two different regimes. (b) Squared radius of gyration $R^2_{\mathrm{gyr}}(e)$ versus energy.

face [from AG to the desorbed globular (DG) bulk phase] and disentangles at even higher temperatures [from DG to the desorbed expanded bulk phase (DE)]. In the latter case, the polymer expands while it is still on the surface (from AG/AG1 to AE) and desorbs at higher temperatures (from AE to DE). The collapse transition in the adsorbed phase takes place at a lower temperature compared to the desorbed phase because the deformation at the substrate leads to an effective reduction of the number of contacts.

Fig. 4(a) reveals a convex regime at the adsorption transition in the microcanonical entropy $s(e)$ for extended chains. Hence, the adsorption transition of non-grafted chains is first-order like for finite chains. This convex intruder vanishes for longer chains[20] such that the continuous behaviour is regained in the thermodynamic limit.

Grafted Polymer. The grafting mainly has an influence on the adsorption transition. Fig. 3(b), e.g., reveals that it is strongly weakened for all ϵ_s, and Fig. 4 shows why this is so. The offset between the microcanonical entropy $s(e) = \ln g(e)/N$ of grafted and non-grafted polymers at high temperatures in Fig. 4(a) is proportional to the translational entropy difference of the two cases[20]. Due to the grafting, the translational entropy for desorbed chains is strongly reduced such that no convex intruder occurs for grafted chains and hence the adsorption of finite extended grafted polymers is continuous. Fig. 4(b) provides additional information about the conformational entropy. Directly at the adsorption transition, the overall radius of gyration gets reduced for non-grafted polymers compared to grafted ones if ϵ_s has a value large enough for the adsorption transition temperature to exceed the collapse transition. Conformations with such a reduced overall size – the same size that is on average adopted in bulk solution at this energy – are the transition states of the phase coexistence. Grafted chains are influenced by the surface in all cases, because they cannot escape. Hence, the conformational rearrangement of extended non-grafted polymers upon adsorption is not necessary and the adsorption is continuous.

The case of globular chains has to be discussed separately. While non-grafted globu-

Figure 5. (a) Specific heat $c_V(T)$, (b) fluctuation of the radius of gyration component perpendicular to the substrate $d\langle R_{\mathrm{gyr},\perp}\rangle(T)/dT$, and (c) fluctuation of the number of monomers in contact with the substrate $d\langle n_s\rangle(T)/dT$ for weak surface attraction, $\epsilon_s = 0.7$, where the adsorption occurs at a lower temperature than the collapse.

lar chains adsorb continuously here, for grafted globular chains it even is nontrivial to identify an adsorption transition. A globular chain attached to a substrate always has several surface contacts such that a "desorbed globule" stops to be a well-defined description
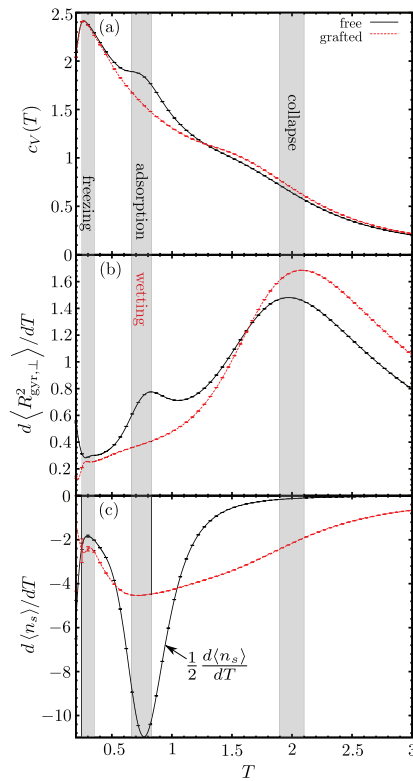
here. One might, however, identify the transition from attached globules that only have a few contacts to docked conformations for stronger surface attraction strengths with the wetting transition. This roughly coincides with the position of the adsorption transition for the free chain between DG and AG in the phase diagram and is illustrated for $\epsilon_s = 0.7$ in Fig. 5. For the free polymer, at the adsorption transition a peak is visible in $c_V(T)$, $d\left\langle R^2_{\mathrm{gyr},\perp} \right\rangle / dT$ and $d\left\langle n_s \right\rangle / dT$. For the grafted polymer, the first two peaks disappear and with it the adsorption transition. Only a signal in the number of surface contacts is left. This change of surface contacts in an otherwise unchanged attached globule signals the wetting transition.

5 Conclusion

By using extensive parallel tempering simulations, we have analyzed and compared the whole phase diagram of a generic off-lattice model for grafted and non-grafted polymer chains for a range of temperatures and surface interaction strengths. The main differences were found at the adsorption transition. Here, the restriction of translational entropy due to grafting is much stronger above than below the transition. Additionally, grafting reduces the necessary rearrangement of segments to form substrate contacts and to adsorb such that grafted adsorption is always continuous whereas the adsorption of the free chain exhibits first-order like signatures for strong surface attraction and short chains. When for grafted chains, the adsorption temperature is below the coil-globule transition temperature, there are always several surface contacts present and the adsorption changes into the wetting transition. For free chains, a continuous adsorption transition exists here.

Acknowledgements

References

1. W. Paul *et al.*, *Unexpectedly normal phase behavior of single homopolymer chains*, Phys. Rev. E **75**, 060801 (2007).
2. T. Vogel, M. Bachmann, and W. Janke, *Freezing and collapse of flexible polymers on regular lattices in three dimensions*, Phys. Rev. E **76**, 061803 (2007).
3. M. P. Taylor, W. Paul, and K. Binder, *All-or-none proteinlike folding transition of a flexible homopolymer chain*, Phys. Rev. E **79**, 050801 (2009).
4. F. Kuhner, M. Erdmann, and H. E. Gaub, *Scaling exponent and Kuhn length of pinned polymers by single molecule force spectroscopy*, Phys. Rev. Lett. **97**, 218301 (2006).
5. M. Bachmann *et al.*, *Microscopic mechanism of specific peptide adhesion to semiconductor substrates*, Angew. Chem. Int. Ed. **122**, 9721 (2010).

6. D. E. Smith *et al.*, *The bacteriophage Φ29 portal motor can package DNA against a large internal force*, Nature **413**, 748 (2001).

7. K. Kegler, M. Salomo, and F. Kremer, *Forces of interaction between DNA-grafted colloids: An optical tweezer measurement*, Phys. Rev. Lett. **98**, 058304 (2007).

8. E. Eisenriegler, K. Kremer, and K. Binder, *Adsorption of polymer chains at surfaces: Scaling and Monte Carlo analyses*, J. Chem. Phys. **77**, 6296 (1982).

9. Z. Usatenko, *Adsorption of long flexible polymer chains at planar surfaces: scaling analysis and critical exponents*, J. Stat. Mech. Theor. Exp. **2006**, P03009 (2006).

10. J. Forsman and C. E. Woodward, *Prewetting and layering in athermal polymer solutions*, Phys. Rev. Lett. **94**, 118301 (2005).

11. R. Rajesh *et al.*, *Adsorption and collapse transitions in a linear polymer chain near an attractive wall*, Phys. Rev. E **65**, 056124 (2002).

12. J. Luettmer-Strathmann *et al.*, *Transitions of tethered polymer chains: A simulation study with the bond fluctuation lattice model*, J. Chem. Phys. **128**, 064903 (2008).

13. S. Metzger *et al.*, *Surface excess in dilute polymer solutions and the adsorption transition versus wetting phenomena*, J. Chem. Phys. **118**, 8489 (2003).

14. J. Krawczyk *et al.*, *Layering transitions for adsorbing polymers in poor solvents*, Europhys. Lett. **70**, 726 (2005).

15. M. Bachmann and W. Janke, *Conformational transitions of nongrafted polymers near an absorbing substrate*, Phys. Rev. Lett. **95**, 058102 (2005); *Substrate adhesion of a nongrafted flexible polymer in a cavity*, Phys. Rev. E **73**, 041802 (2006).

16. T. Vrbová and S. G. Whittington, *Adsorption and collapse of self-avoiding walks in three dimensions: A Monte Carlo study*, J. Phys. A **31**, 3989 (1998).

17. R. Hegger and P. Grassberger, *Chain polymers near an adsorbing surface*, J. Phys. A **27**, 4069 (1994).

18. Y. Singh, D. Giri, and S. Kumar, *Crossover of a polymer chain from bulk to surface states*, J. Phys. A **34**, L67 (2001).

19. M. Möddel, M. Bachmann, and W. Janke, *Conformational mechanics of polymer adsorption transitions at attractive substrates*, J. Phys. Chem. B **113**, 3314 (2009).

20. M. Möddel, W. Janke, and M. Bachmann, *Systematic microcanonical analyses of polymer adsorption transitions*, Phys. Chem. Chem. Phys. **12**, 11548 (2010).

21. M. Möddel, W. Janke, and M. Bachmann, *Comparison of the adsorption transition for grafted and non-grafted polymers*, preprint (2011).

22. W. A. Steele, *The physical interaction of gases with crystalline solids*, Surf. Sc. **36**, 317 (1973).

23. K. Hukushima and K. Nemoto, *Exchange Monte Carlo method and application to spin glass simulations*, J. Phys. Soc. Japan **65**, 1604 (1996).

24. D. J. Earl and M. W. Deem, *Parallel tempering: Theory, applications, and new perspectives*, Phys. Chem. Chem. Phys. **7**, 3910 (2005).

25. E. Bittner, A. Nußbaumer, and W. Janke, *Make life simple: Unleash the full power of the parallel tempering algorithm*, Phys. Rev. Lett. **101**, 130603 (2008).

26. A. M. Ferrenberg and R. H. Swendsen, *Optimized Monte Carlo data analysis*, Phys. Rev. Lett. **63**, 1195 (1989).

27. M. K. Fenwick, *A direct multiple histogram reweighting method for optimal computation of the density of states*, J. Chem. Phys. **129**, 125106 (2008).